IOP Publishing Nanotechnology
Nanotechnology 28 (2017) 395702 (12pp) https://doi.org/10.1088/1361-6528/aa87d0

Probing of free and localized excitons and trions in atomically thin WSe_2, WS_2, $MoSe_2$ and MoS_2 in photoluminescence and reflectivity experiments

J Jadczak[1,4], J Kutrowska-Girzycka[1], P Kapuściński[1], Y S Huang[2], A Wójs[3] and L Bryja[1]

[1] Department of Experimental Physics, Wroclaw University of Science and Technology, Wroclaw, Poland
[2] Department of Electronic Engineering, National Taiwan University of Science and Technology, Taipei 106, Taiwan
[3] Department of Theoretical Physics, Wroclaw University of Science and Technology, Wroclaw, Poland

E-mail: joanna.jadczak@pwr.edu.pl

Received 3 July 2017, revised 14 August 2017
Accepted for publication 23 August 2017
Published 6 September 2017

Abstract

We report on detailed temperature dependent (T = 7–295 K) optical spectroscopy studies of WSe_2, WS_2, $MoSe_2$ and MoS_2 monolayers exfoliated onto the same SiO_2/Si substrate. In the high energy region of absorption type (reflectivity contrast—RC) and emission (photo-luminescence—PL) spectra of all the monolayers resonances related to the neutral and charged excitons (X and T) are detected in the entire measured temperature range. The optical amplitudes of excitons and trions strongly depend on the temperature and two dimensional carrier gas (2DCG) concentration. In the low energy PL spectra of WSe_2 and WS_2 we detect a group of lines (L) which dominates the spectra at low temperatures but rapidly quenches with the increase in the temperature. Interestingly, in the same energy range of the RC spectra recorded for WS_2, we observe an additional line (L_0), which behaves in the same way as the L lines in the PL spectra. The optical amplitude of L_0 and T resonances in the RC spectra strongly increases with the growth of the 2DCG concentration. On the base of these observations we identify the L_0 resonance in the RC spectra as arising from the fine structure of the trion. We also propose that the line interpreted previously in PL spectra of WSe_2 and WS_2 as related to the biexciton emission is a superposition of the biexciton, trion and localized exciton emission. We find that with the temperature increase from 7–295 K the total PL intensity decreases moderately in WSe_2 and WS_2, strongly in MoS_2 and dramatically in $MoSe_2$.

Keywords: transition metal dichalcogenides monolayers, excitons, trions, localized excitons

(Some figures may appear in colour only in the online journal)

1. Introduction

Semiconducting transition metal dichalcogenides (TMDCs) of chemical formula MX_2 (such as WSe_2, WS_2, $MoSe_2$ and MoS_2) have attracted considerable attention from the scientific community due to the underlying physics and promising applications in photonics, optoelectronics and the development of valleytronics [1–12].

Similarly to graphene, in monolayers of TMDCs the bottom of the conduction band and the top of the valence band are located at the binary indexed corners K_+ and K_- of the 2D hexagonal Brillouin zone. On the other hand, contrary to graphene, the lack of inversion symmetry and a strong spin–orbit coupling in single layers of TMDCs results in valley-contrasting strong spin splitting of the valence and

[4] Author to whom any correspondence should be addressed.

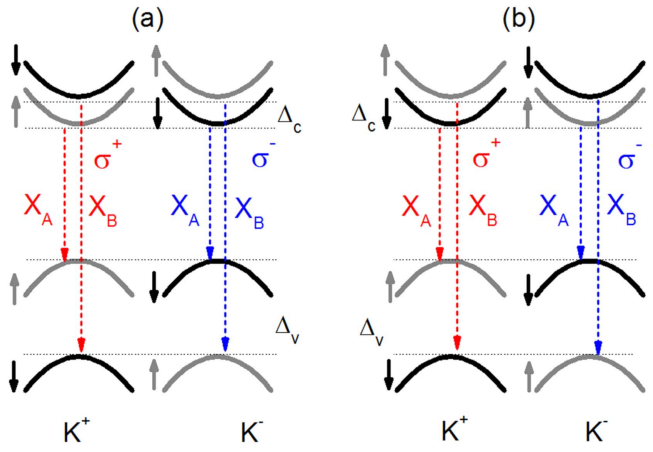

Figure 1. A diagram of low energy subbands in the conduction and valence bands at the K^+ and K^- points of the 2D Brillouin zone of: (a) molybdenum based TMDC and (b) tungsten based TMDC. The spin-up (spin-down) subbands are denoted in gray (black) colors. Δ_c and Δ_v indicate the corresponding spin–orbit splittings of the conduction and valence bands. The optical transitions of A and B excitons active in σ^+ and σ^- helicities are indicated by red and blue dashed arrows, respectively.

conduction bands. The confinement to a single layer and reduced dielectric screening lead to strong many body effects mediated by Coulomb interactions. In the TMDC monolayers, excitons, bound electron–hole pairs ($X = e + h$) exhibit very high binding energies of a few hundreds of meV [13–15], which leads to their stability at room temperature. In the presence of excess carriers charged excitons, trions (T), consisting of two electrons and one hole or two holes and one electron, are detected in optical spectra of TMDC monolayers [16–29]. The spin splitting of the valence band Δ_v, leading to formation of so called A and B excitons, amounts to about 150, 180, 430, and 450 meV for the MoS_2, $MoSe_2$, WS_2, and WSe_2 monolayer, respectively [30]. A diagram of relevant subbands in the conduction and valence bands at the K^+ and K^- of the 2D hexagonal Brillouin zone of MoS_2, $MoSe_2$, WS_2, and WSe_2 is presented in figure 1. As predicted in theoretical calculations [6, 31], the conduction-band spin splitting Δ_c is significantly smaller and shows a larger relative variance between different TMDC monolayers. It leads to the splitting between the dark and bright exciton subbands of the so-called A-exciton defined by the spin–orbit splitting in the conduction band, Δ_c. Bright excitons are composed of an electron and hole with parallel spin, whereas dark excitons are composed of the electron and hole with the opposite spin. In molybdenum based TMDC Δ_c is predicted to be positive (equals 3 and 21 meV in MoS_2 and $MoSe_2$, respectively), resulting in the lowest energy exciton subband being bright (figure 1(a)). In contrast, in tungsten based TMDC Δ_c is predicted to be negative (equals −32 and −37 meV in WS_2 and $MoSe_2$, respectively), and the lowest energy subband is dark (figure 1(b)). In the low temperature PL spectra of selenides ($MoSe_2$ and WSe_2) monolayers, well resolved exciton and trion transitions are detected [16–22]. However, the emission spectra of sulfides (MoS_2 and WS_2) monolayers reveal different character, with larger broadening, and observation of the fine structure of exciton and trion often requires special conditions, e.g. applying gating or alternatively choosing samples with appropriate doping levels [24–26]. The differences in the PL spectra between selenides and sulfides monolayers are mainly related to the substantial difference of their intrinsic two dimensional (2D) carrier concentration (measured in vacuum), which in sulfides is about two orders of magnitude higher than in selenides [4, 16]. Low temperature emission spectra of WSe_2 and WS_2 are dominated by lines positioned in the low energy sector of PL spectra. The nature of these lines is still under debate. They have been assigned to excitons localized on defects (L) [17, 24–29] or to indirect excitons [31]. You *et al* [27] reported on observation of biexciton emission (XX) in the low temperature PL spectra of a WSe_2 monolayer. Their interpretation was based on the superlinear dependence of emission intensity from the XX species with respect to the X emission in excitation power dependent experiments and quenching of the XX line for the lowest excitation power densities. Plechinger *et al* [25, 26] reported on the observation of biexciton emission in a WS_2 monolayer. However, they claimed that the XX emission merged with the emission of a localized exciton (L). They measured a linear increase in the integrated XX/L PL intensity for low excitation densities and a quadratic one for higher exciton densities, which in their interpretation is related to two different emission lines: at low excitation density, the main contribution to the PL peak stems from defect-bound excitons, and at high excitation density, the biexciton (XX) emission is dominant. However, other authors reported experiments in favor of a trion nature of this species. Jones *et al* [28] showed in PL experiments on a WSe_2 monolayer that by applying a gate voltage, the spectral weight of PL transfers from the neutral exciton (X) to the trion (T) and at a voltage higher than 20 V, to a new PL feature (named X2′), positioned at the same energy as the biexciton emission reported in [27]. They show that X2′ behaves in the same way as the trion, and suggest that X2′ probably arises from the fine structure of the trion. The well resolved X and T resonances have been also observed in the RC spectra of most TMDCs [14, 18, 19] but to the date the observation of an additional low energy line in the RC spectra has not been reported.

The aim of this paper is to clarify this issue, and to gain insight into the nature of excitons observed in different energy regions of the optical spectra of TMDCs. We present detailed optical spectroscopy studies of WSe_2, WS_2, $MoSe_2$ and MoS_2 monolayers exfoliated onto the same SiO_2/Si substrate. In the high energy region of absorption type (reflectivity contrast) and emission (photoluminescence) spectra of all the monolayers we detect two resonances of the neutral and charged excitons (X and T), whose optical amplitudes strongly depend on the temperature and two dimensional carrier gas (2DCG) concentration. In the low energy PL spectra of WSe_2 and WS_2 we detect a group of lines (L) which dominates the spectra at low temperatures but rapidly quenches with the increase in the temperature. Surprisingly, an additional line (L_0) which we detected at the low energy RC spectra of the WS_2 monolayer exhibits similar temperature behavior as the L lines in the PL spectra. The optical amplitude of the L_0 and T resonances in the RC spectra strongly increases with the increase in the 2DCG concentration. On the

base of these observations we identify the L_0 resonance in the RC spectra as arising from the fine structure of the trion. We also propose that the line interpreted previously in PL spectra of WSe_2 and WS_2 as related to the biexciton emission is a superposition of the biexciton, trion and localized exciton emission. We find that the total PL intensity at all measured temperatures is the highest for WSe_2. We also observe that with the temperature increase from 7 to 295 K the total PL intensity decreases moderately in WSe_2 (≈5×) and WS_2 (≈7×), strongly in MoS_2 (≈40×) and dramatically in $MoSe_2$ (≈1000×). Our observations contrast with the previous reports, where the increase in the total PL intensity for WSe_2 with the increase in the temperature was reported. We attribute this contrasting temperature evolution of the total PL intensity of WSe_2 to the different 2D carrier concentration in the investigated monolayers.

2. Methods

The studied monolayers of WSe_2, WS_2, $MoSe_2$ and MoS_2 were prepared by mechanical exfoliation of bulk crystals grown by the chemical vapor transport technique. Prior to the crystal growth, powdered compounds of the series were prepared from the elements (Mo: 99.99%; W: 99.99%, S: 99.999%; Se: 99.995%) by reaction at $T = 1000\,^{\circ}\mathrm{C}$ for 10 d in evacuated quartz ampoules. The chemical transport was achieved with Br_2 as a transport agent in the amount of about $5\,\mathrm{mg\,cm^{-3}}$. Initially, flakes were exfoliated onto DGL film (Gel-Pak), attached to a glass plate and identified by their optical contrast and characterized by Raman scattering and PL measurements at 295 K. For further optical studies, they were deposited on the same Si/SiO_2 (295 nm) target substrate.

The samples were mounted on a cold-finger of a non-vibrating closed cycle cryostat, where temperature can be varied from 6 to 300 K. Photoluminescence was excited by the 532 nm (2.33 meV) line of a Diode-Pumped Solid State laser. The laser beam was focused on the sample under normal incidence using a 50× magnification long working distance microscope objective (NA = 0.65). The diameter of an excitation spot was equal to ≈1.5 μm. PL signal was collected by the same objective. The spectra were analyzed with an 0.5 m focal length spectrometer with a 600 lines $\mathrm{mm^{-1}}$ grating. A Peltier-cooled Si charge couple device was used as a detector. The RC measurements were conducted in the same set-up with filament lamp as a light source.

3. Results and discussion

In figure 2 examples of comparative PL and RC spectra of all the studied monolayers are presented at $T = 7$ K. In PL measurements the laser excitation power is kept relatively low at $P = 80\,\mu$W to avoid possible heating effects. Two resonances are observed in the higher energy region of the PL and RC spectra for all the samples. We attribute them to the optical transitions of an exciton (X, a higher-energy one) and trion (T, a lower-energy one). The energy position of X and T resonances are in good agreement with the previous reports [16–29]. The exciton and trion energies, as well as their full widths at half maximum (FWHM), for all the studied monolayer are presented in table 1.

The common feature observed in the PL spectra of all the studied monolayers is that the PL intensity of the trion exceeds that of the exciton. In contrast, in reflectivity spectra of selenides, WSe_2 and $MoSe_2$, the exciton resonance is substantially stronger than that of the trion. Moreover, in WSe_2 the trion resonance is scarcely distinguished in the RC spectra. In the RC spectra of WS_2 the X resonance is slightly stronger than the T resonance, and only in MoS_2 the T resonance is stronger than that of X. The reason for the difference in the optical amplitude of the exciton and trion in the PL and RC spectra is that the strength of the exciton and trion resonances in reflectivity is determined by respective density of states, whereas the PL intensity is contributed additionally by a state occupation factor. At low temperatures, the excess carriers and photo-created excitons (electron–hole pairs) thermalize to the same locations, corresponding to the minima of the potential in the monolayer, leading to the increase in the probability of the trion formation that is observed as an increase in the trion emission relative to the exciton emission. The relation in the strength of the exciton and trion resonances in the RC spectra depends on the 2DCG concentration. The increase in the 2DCG concentration results in the increase in the strength of the trion resonance relative to the strength of the exciton resonance. An inspection of the RC spectra presented in figure 4 shows that the lowest 2DCG concentration is expected in WSe_2, whereas the highest in MoS_2. Also, the 2DCG concentration in the studied monolayers is higher in sulfides than in selenides, that is in agreement with the previous reports, where about two orders of magnitudes higher 2DCG concentration in the sulfides than in the selenides was measured [4, 16]. The FWHM of the exciton and trion lines is about two times higher in the sulfides than in the selenides, that also points to its relation with the 2DCG concentration. In the low energy sector of the PL spectra of the tungsten compounds shown in figures 1(a) and (b) a group of high intensity lines (L_1–L_5) in WSe_2 and (L_1–L_4) in WS_2 is detected. In the RC spectra of WS_2 presented in figure 1(a) we observe a new, additional line (named L_0). To the date this line has not been observed.

The strength of the L_0 resonance is strongly position dependent. In figure 3 the RC spectra of the WS_2 monolayer recorded at different points on the monolayer are presented. As is seen there is a clear correlation between the strength of the X, T and L_0 resonances. The increase in the strength of the L_0 resonance is accompanied by the simultaneous increase in the strength of the T resonance and the decrease of the strength of the X resonance. Since the increase in the trion strength relative to the exciton strength is related to the increase in the 2DCG concentration, this observation implies that: (1) the concentration of the 2DCG is different in different regions of the studied WS_2 monolayer, and (2) the strength of the L_0 resonance increases with the increase in the 2DCG concentration. The observed increase in the strength of the T and L_0 resonances in the RC spectra with the increase in the 2DCG concentration allows us to assess both features as related to the fine structure of the trion. It is well established

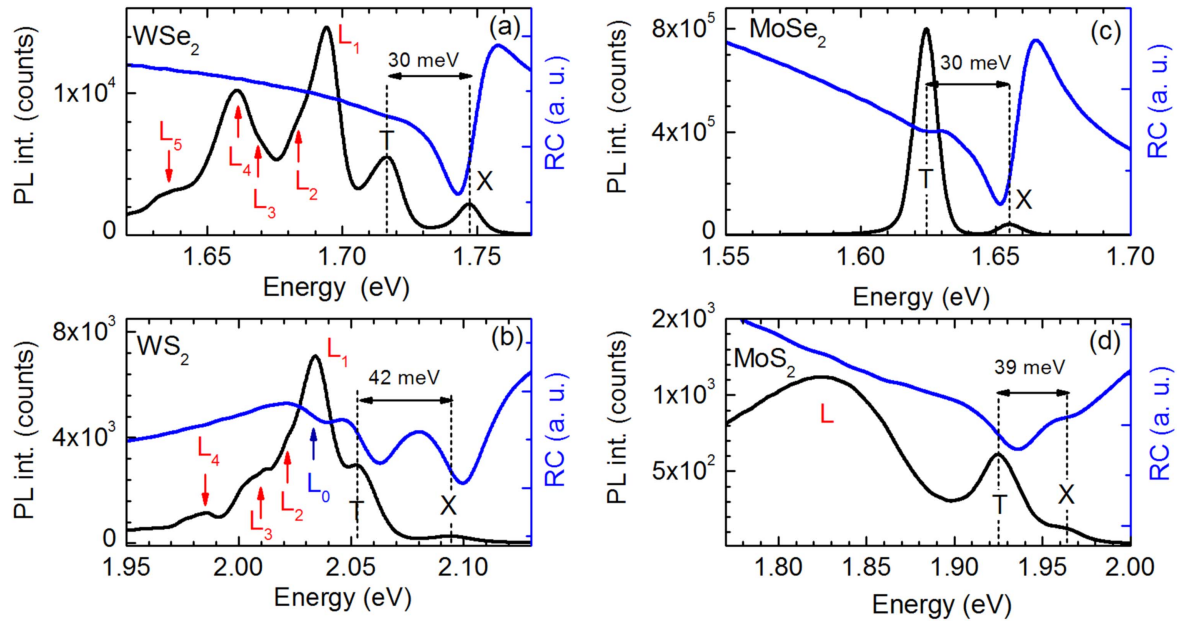

Figure 2. Examples of comparative PL and RC spectra recorded at $T = 7$ K for the monolayers of: (a) WSe_2, (b) WS_2, (e) $MoSe_2$, (g) MoS_2.

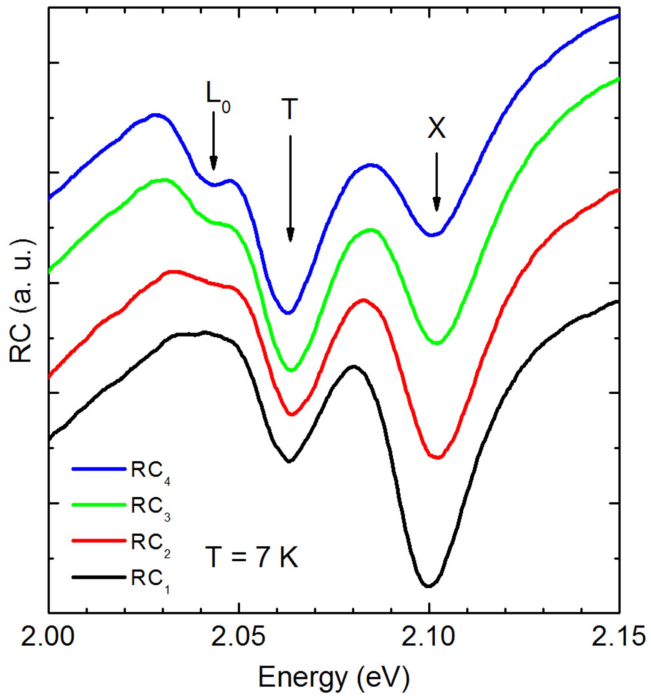

Figure 3. The RC spectra of WS_2 recorded at different points on a monolayer. Spectra are ordered from low strength of the L_0 resonance at the bottom (RC_1) to high strength at the top (RC_4).

Table 1. Energies and full widths at half maximum (FWHM) of excitons and trions measured in the PL spectra at $T = 7$ K for all the studied monolayers.

	WSe_2	$MoSe_2$	WS_2	MoS_2
E_X (eV)	1.747	1.655	2.097	1.964
FWHM (meV)	10	10	18	18
E_T (eV)	1.716	1.625	2.055	1.925
FWHM (meV)	12	11	20	20

from the PL studies of gated WS_2 structures that pristine WS_2 MLs are n-type doped, so we attribute the T and L_0 resonances to two optically bright negatively charged trion species (X^-). Due to the Pauli principle two constituent electrons in a trion in TMDC monolayers occupy states with different spin or valley index. In a WS_2 monolayer this leads to three possible pairs of doubly degenerate configurations of the bright trion X^- complex, schematically presented in figure 4: (a) the intravalley trion, with a hole and a pair of electrons in the same valley in the upper and lower conduction bands, forming an electron spin singlet state, (b) the intervalley trion, with electrons located in different valleys, in the upper and lower conduction bands, forming an electron spin triple state, and (c) the intervalley trion with electrons located in different valleys, but in the upper conduction bands, forming an electron triplet state. Due to the opposite spin splitting of the valence and conduction bands in WS_2, the optical selections rules, for optically bright trions, enforce a recombination of an electron in the higher-energy spin-split conduction band with a hole in the same valley.

The formation of trion complexes with an additional electron in the lower-energy spin-split conduction band, presented in figures 4(a) and (b), are more probable at low two-dimensional electron gas (2DEG) concentrations, whereas the formation of the trion complex with electrons in the higher-energy spin-split conduction bands are preferable at higher 2DEG concentrations, when the electron Fermi level is located above the upper spin-split conduction band. Further in the text we will determine for our WS_2 monolayer the electron Fermi level $E_F = 12$ meV, which is equal roughly to one half of theoretically predicted energy distance between spin-split conduction bands. One possible model that could explain the coexistence of the T and L_0 resonances in the RC spectra is that the WS_2 monolayer is inhomogeneous, possibly due to interaction with the substrate or randomly created vacancies. This results in distinct regions: (1) regions with

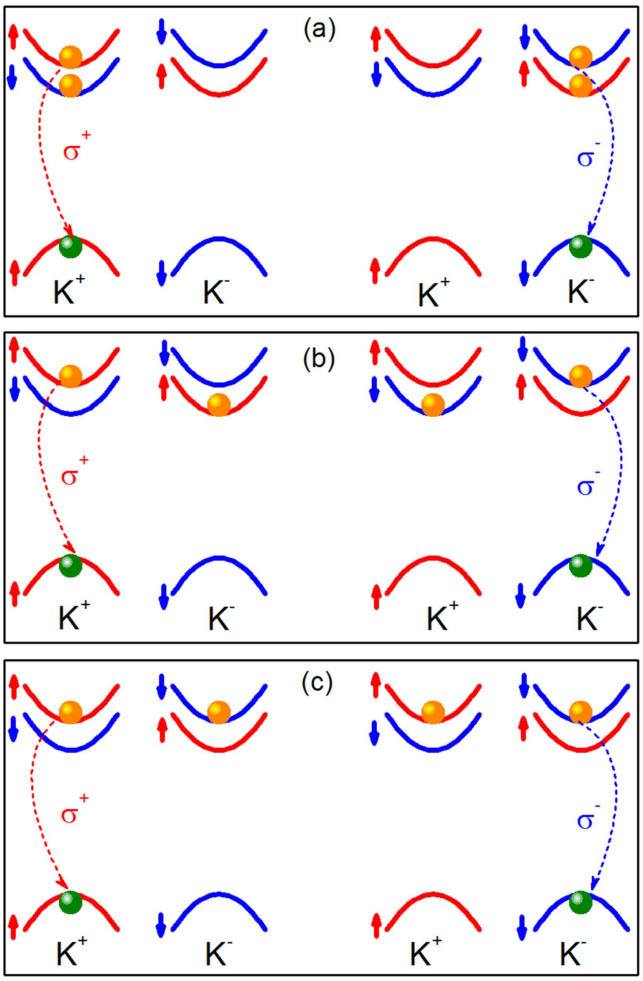

Figure 4. A schematic illustration of possible configurations of a hole and a pair of electrons in a bright negatively charged A exciton (trion) in a WS_2 monolayer at the K^+ and K^- points of the 2D Brillouine zone. The spin-up (spin-down) subbands are denoted in red (blue) colors. The electrons (holes) in the conduction (valence) band are represented by orange (green) spheres.

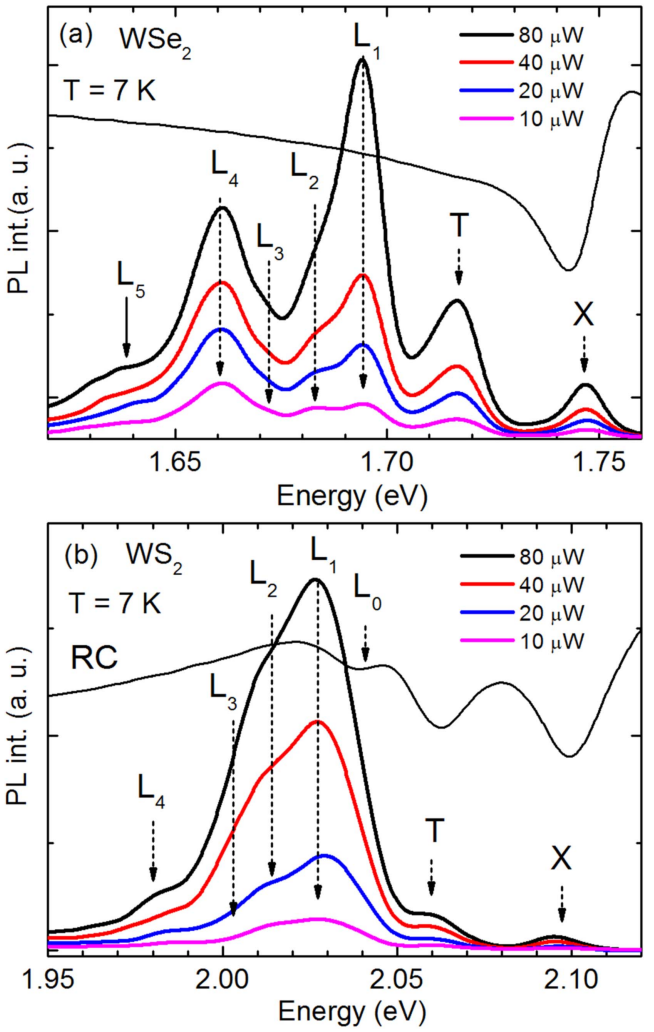

Figure 5. Evolution of the PL spectra as a function of the excitation power, recorded at $T = 7$ K, for (a) WSe_2 and (b) WS_2.

low 2DEG concentration, for which we detect only X and T resonances, and (2) regions with high 2DEG concentration and the electron Fermi level positioned above the upper spin-split conduction band, for which we detect all three X, T and L_0 resonances. Our interpretation of the fine structure of the trion in WS_2 monolayer predicts energy splitting of the trion into three separate resonances, not resolved within the line-width of the T and L_0 features in our RC spectra. However, in the previous studies of the low temperature PL spectra of WS_2 monolayer Plechinger *et al* [26] have observed the energy splitting of the T feature into two components, which they attributed to the electron spin singlet and triplet states, with an additional electron in the lower conduction band (figures 4(a) and (b), respectively). The splitting of the singlet–triplet states equal to 11 meV observed in [26] is more than two times smaller than the one observed in our RC spectra, where the splitting between the T and L_0 resonances is equal to 24 meV. Our interpretation implies that the binding energy of the trion with two electron in the upper conduction bands is higher than that of the trion with one electron in the upper and one in the lower conduction bands. This interpretation needs confirmation in further theoretical studies.

Let us discuss now the nature of the low energy peaks, L_1–L_5 and L_1–L_4 observed in the PL spectra of WSe_2 and WS_2 (figures 2(a) and (b), respectively). As is seen in figure 2(b), the PL lines: X, T and L_1 are red shifted, by about 5 meV, in respect to the RC resonances: X, T and L_0, respectively. This observation suggests the similar character of the L_0 and L_1 features. However, in the previous studies the L_1 feature in PL spectra of WS_2 was attributed to the superposition of biexciton and localized exciton emission [25]. To gain more insight into the character of the L_1 and other low energy L lines we performed excitation power dependent PL measurements of WS_2 and WSe_2 monolayers.

In figures 5(a) and (b) the respective PL spectra of WSe_2 and WS_2 monolayers recorded at $T = 7$ K, for different excitation powers, are presented. At low excitation powers all the X, T and L lines in the PL spectra of WSe_2 are well separated and have comparable intensities, whereas at higher excitation powers the L_1 line strongly dominates the spectra. In the PL spectra of WS_2 only the X and T lines are well

separated, whereas the L_1 line merges with the lower energy L_2–L_4 lines. However, the same relation in the evolution of the total PL intensity of the X, T, L_1 and L_2–L_4 species as a function of the excitation power is observed. The common feature observed in the evolution of the PL spectra of both monolayers as a function of the excitation power is that the integrated PL intensity of the exciton and trion grows almost linearly, whereas the integrated PL intensity of the L_1 exhibits superlinear growth with the excitation power. The lines L_2–L_5 in WSe_2 and L_2–L_4 in WS_2 grow sublinearly with the excitation power.

To compare our data with the previous reports [25, 27] we analyze the emission from the L_1 in terms of the neutral exciton X strength using a power law relation of the form $I_{L1} \sim I_X^{\alpha}$. For WSe_2 we obtain $\alpha = 1.28$, slightly lower than $\alpha = 1.39$ obtained in [27]. For WS_2 we obtain $\alpha = 1.46$, whereas in [25] authors report on a linear dependence of the total PL intensity of the relevant line for low excitation powers and a quadratic one for higher excitation powers. They have interpreted this effect as related to emission of two different species with the same PL energy: at low excitation power the main contribution to PL stems from defect bound excitons, whereas for higher excitation powers the emission from biexciton dominates. Although the relation of the L_1 feature in PL spectra of WSe_2 and WS_2 to biexciton emission, proposed in the previous studies, is convincing, on the base of our study of the PL and RC spectra of WS_2 monolayer we propose an alternative interpretation of the L_1 feature as related to the superposition of: biexciton, defect bound exciton and trion emission. However, due to the large broadening of the L_1 feature in the PL spectra of our WS_2 monolayer these three species cannot be resolved in the spectra, even at the lowest laser excitation power $P = 10\ \mu$W (0.35 kW cm^{-2}) applied in our experiment. In our defected and highly electron doped samples the L_1 emission can be contributed by radiative recombination of excitons bound on neutral and charged donors or acceptors. As was shown in theoretical calculations [32, 33], point defects in TMDC serve as both, donors or acceptors. In strongly confined systems in 2D structures, in the presence of an excess electron (hole) gas, a neutral donor, D^0 (or a neutral acceptor, A^0) can bind an additional electron (hole) to form a charged complex D^- (or A^+). In our previous studies we have shown that such charged complexes are stable at low temperatures in 2D $GaAs/Al_xGa_{1-x}$ as semiconductor structures [34, 35]. The stability of such charged complexes is also expected in TMDC monolayers, where the confinement is much stronger than in 2D $GaAs/Al_xGa_{1-x}As$ structures. Indeed, in recent theoretical calculation Ganchev *et al* [36] have shown that in TMDCs such as WSe_2, WS_2, $MoSe_2$ and MoS_2, the binding energy of an additional electron (hole) to a neutral donor (acceptor) is equal to about 30 meV. In a highly n-type doped WS_2 monolayer the formation of optically active complex of an exciton bound on a negatively charged donor D^-X is very probable. However, the PL intensity of charged and localized exciton complexes in $GaAs/Al_xGa_{1-x}As$ 2D structures is very weak [34, 35] and a similar weak contribution of D^-X emission to PL intensity of WS_2 monolayer is expected. Another scenario, possible in our defected structure, is that the L_1 feature is additionally contributed by emission of excitons bound on neutral donors or acceptors (D^0X and A^0X, respectively). In an n-type structure acceptors are compensated and form an optically inactive negatively charged complex A^-. Under illumination a negative A^- can trap a photo-excited hole to become a neutral complex A^0, which can further bind an exciton X to become an optically active complex. It is well known from the PL studies of bulk crystals that the D^0X and A^0X emission intensities exhibit superlinear dependence on the laser power, and the similar behavior is expected in atomically thin TMDC.

We attribute the L_2–L_4 lines positioned in the PL spectra of WS_2 at lower energies in respect to the L_0 line to optical transitions of: electron to acceptor (e–A^0), hole to donor (h–D^0), and donor to acceptor (D^0–A^0) complexes, as they exhibit similar sublinear growth of the emission strength as a function of the laser power as relevant complexes in bulk crystals [37, 38]. As the L_1 line in the PL spectra of the WSe_2 monolayer behaves in the same way as the L_1 lines in the PL spectra of the WS_2 monolayer as a function of the laser excitation power, we assess both lines as related to the same emission species. Also, we perform similar assessment of the L_2–L_5 lines in the PL spectra of the WSe_2 monolayer as the L_2–L_4 lines in the PL spectra of the WS_2 monolayer.

In order to gain further insight into the nature of all the excitonic complexes detected in the PL and RC spectra we perform temperature dependent ($T = 7$–295 K) measurements of all the studied monolayers, presented in figures 6 and 7 for molybdenum and tungsten based TMDC monolayers, respectively. The corresponding spectrum for each temperature is normalized to the maximum value. The complementary figure 8 presents temperature dependence of the PL intensity of excitons, trions, and L lines for the appropriate energy range indicated in figures 6(a) and (c), and 7(a) and (b), respectively. For clarity, within the L lines only the intensity of the L_1 line is presented separately, whereas the PL intensity of L_2–L_5 lines in WSe_2 (figure 8(a)) and the L_2–L_4 lines in WS_2 (figure 8(b)) are drawn as a total PL intensity.

Let us first analyze the temperature evolution of the PL and RC spectra of the tungsten based compounds. The PL spectra of the WS_2 and WSe_2 monolayers exhibit similar behavior as a function of temperature. With increasing temperature the low energy L peaks rapidly quench and they are not detected in the spectrum at temperatures above 80 K. This rapid quench of the low intensity lines is independent of the excitation power, which is clearly seen in figure 9, where we compare evolution of the low temperature ($T \leqslant 80$ K) PL spectra of WS_2 for different excitation powers, equal to 2.5, 10 and 80 μW (each power shown in a different panel, as indicated). The same effect is observed for WS_2 monolayer (not presented). However, in both monolayers with increasing temperature the PL intensity of the L_1 line decreases much slower than the PL intensity of the other L lines: the L_2–L_5 lines in WSe_2 (figure 8(a)) and L_2–L_4 lines in WS_2 (figure 8(b)). Surprisingly, in the WS_2 monolayer the L_0 resonance in the RC spectra exhibits similar temperature evolution as the L_1 resonance in the PL spectra and disappears

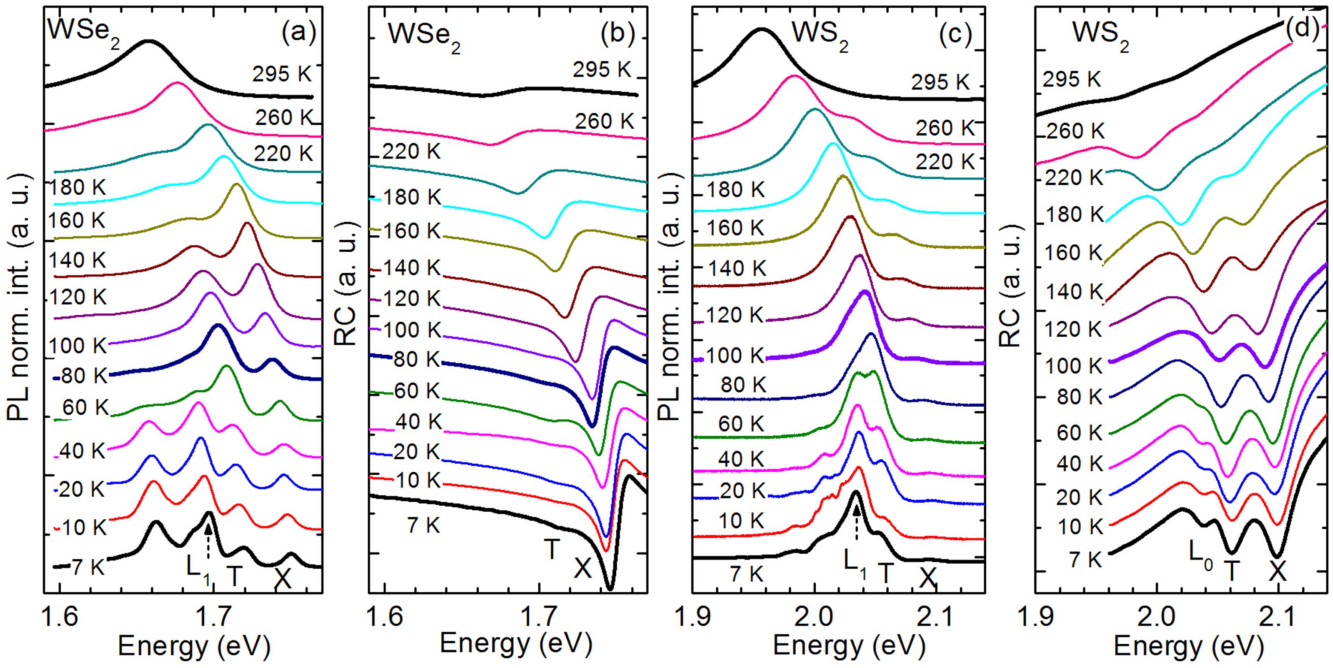

Figure 6. The temperature evolution of the PL and RC spectra of WSe_2 and WS_2 monolayers. (a) PL spectra of WSe_2. (b) RC spectra of WSe_2. (c) PL spectra of WS_2. (d) RC spectra of WS_2.

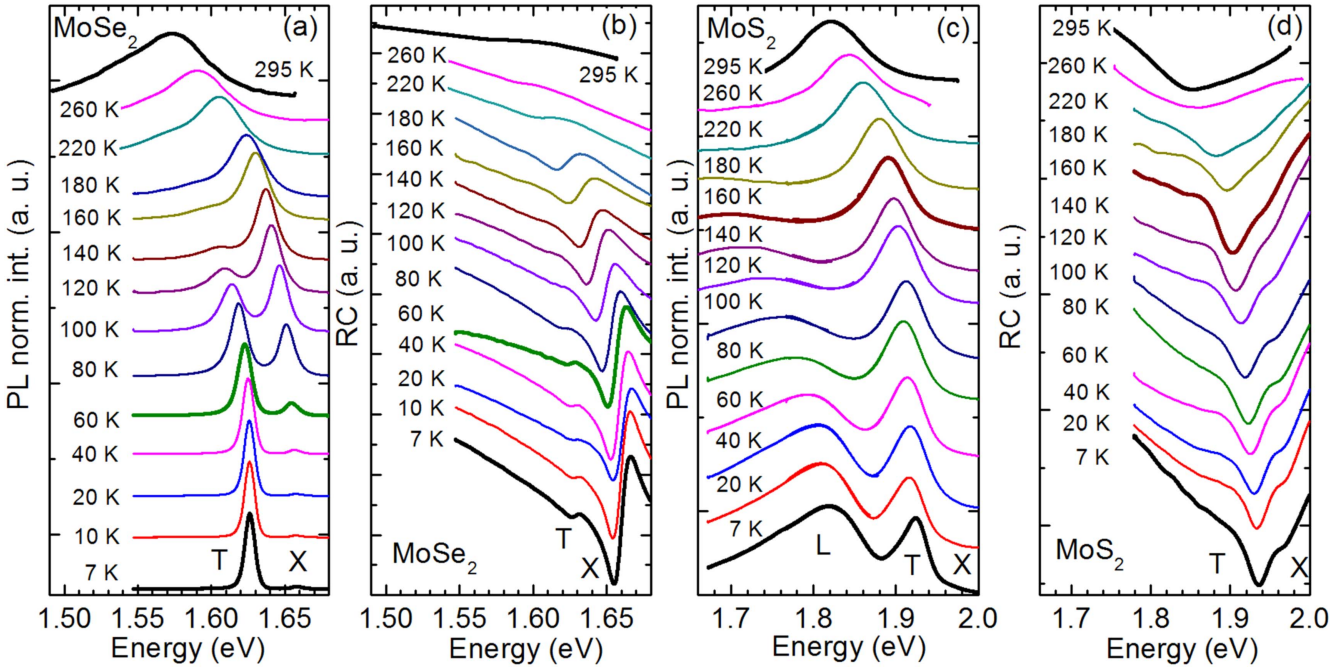

Figure 7. The temperature evolution of the PL and RC spectra of $MoSe_2$ and MoS_2 monolayers. (a) PL spectra of $MoSe_2$. (b) RC spectra of $MoSe_2$. (c) PL spectra of MoS_2. (d) RC spectra of MoS_2.

from the RC spectra spectra at the same temperature $T > 80$ K. This accounts for the relation of the L_0 and L_1 resonance to the same radiative complex. In order to interpret the rapid temperature quenching of the L_0 and L_1 features we consider the impact of the inhomogeneous distribution of the 2DEG in our WS_2 monolayer. The electron Fermi level, evaluated from the overall 2DEG concentration in our sample, equals $E_F = 12$ eV and is roughly located in the middle of the spin-split conduction bands. In our interpretation of the L_0 resonance as related to the negative trion, with a pair of electrons located in the upper spin-split conduction bands, we assume that due to the potential fluctuations in some regions of the monolayer the upper spin-split conduction band is positioned below the Fermi level. As the temperature increases, the access electrons become more mobile, that causes a more homogeneous redistribution of the 2DEG over the whole sample, which in turn leads to decrease of the number of electrons in the upper conduction bands and the L_0

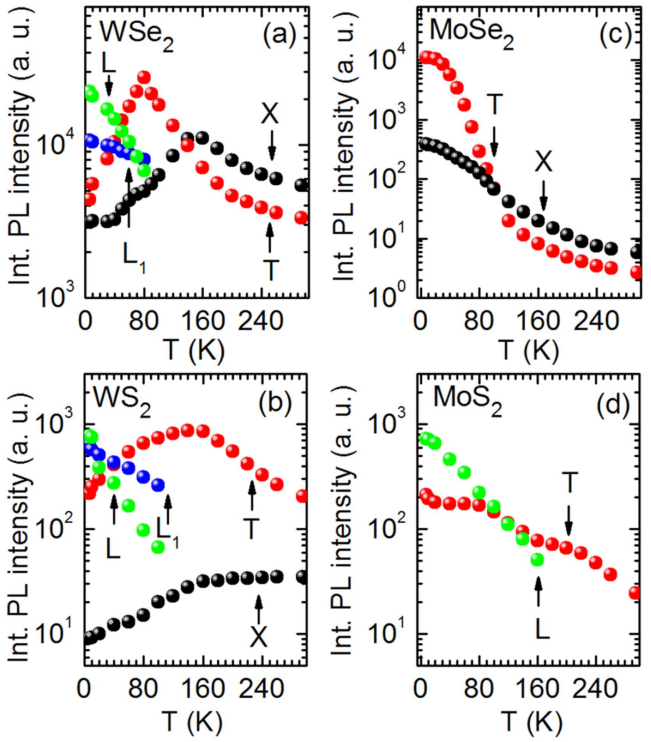

Figure 8. Integrated PL intensities of excitons, trions and localized excitons as a function of the temperature in: (a) WSe_2, (b) WS_2 (c) $MoSe_2$ and (d) MoS_2.

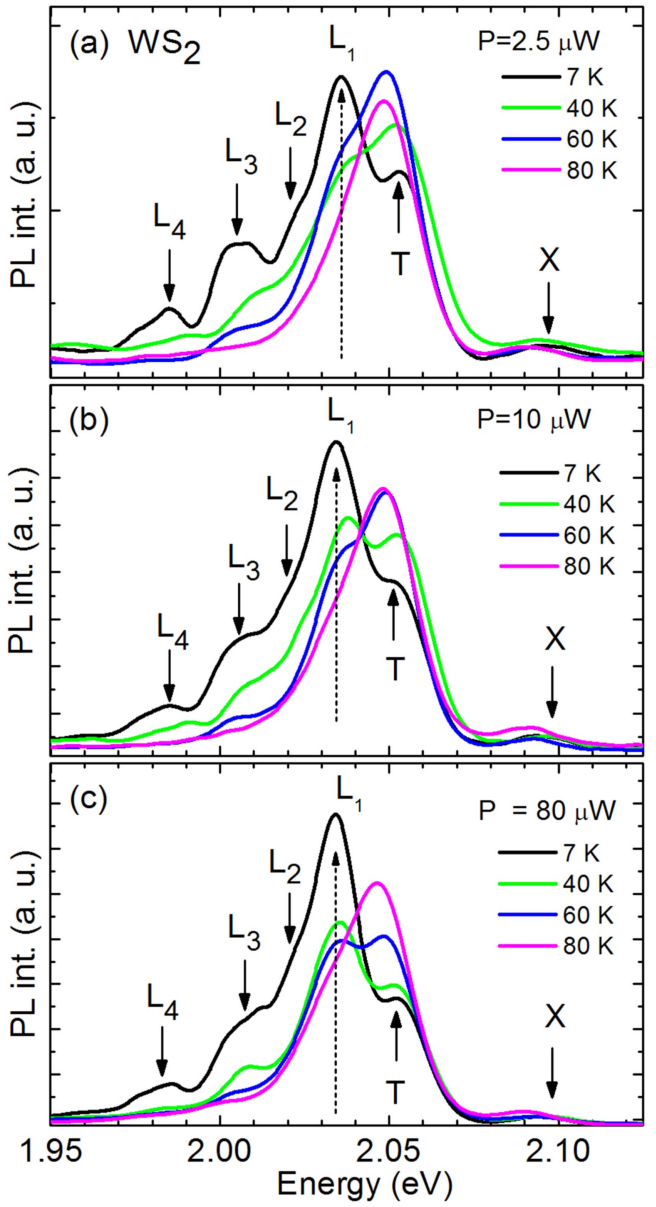

Figure 9. The low temperature ($T \leqslant 80$) evolution of the PL spectra of WS_2 under different excitation powers: (a) $P = 2.5$ μW, (b) $P = 10$ μW, (c) $P = 80$ μW.

resonance disappears from the RC spectra of the WS_2 monolayer. With the increase in the temperature, the occupation of the lower spin-split conduction band is only weakly affected and the T resonance, related to the trion complex with the access electron in the lower spin-split conduction band, is detected in the PL and RC spectra up to $T = 295$ K.

In contrast to low energy L lines the X and T lines contribute to the PL spectra of WS_2 and WSe_2 monolayers at all measured temperatures $T = 7$–295. This is related to a higher oscillator strength of the X and T states compared to the localized states. However, the optical amplitude of X and T resonances strongly differs in the absorption (RC) and emission spectra (PL) of both the WS_2 and WSe_2 monolayers, what is mainly related to the different 2DEG concentrations in sulfides and selenides and, as it has been discussed above, to that fact that the strength of the X and T resonances in reflectivity is determined by respective density of states, whereas the PL intensity is contributed additionally by a state occupation factor.

We observe similar temperature evolution of the X and T resonances in the PL and RC spectra in the $MoSe_2$ and MoS_2 monolayers (figure 7), as in the WSe_2 and WS_2 monolayers (figure 5). The low energy line, detected in the PL spectra of MoS_2 (denoted as L) decreases in intensity with the increase in the temperature, similarly as the L lines in tungsten based compounds, but the L line in MoS_2 quenches at much higher $T > 160$ K, which is likely related to its much higher binding energy in comparison to the L lines in the WS_2 and WSe_2 monolayers. As expected, the X and T resonances in the PL and RC spectra of all the studied monolayers shift to lower energy following the reduction of the band gap at increased temperature [16, 19]. The observation of the X and T resonances in the entire temperature range and the strong temperature induced transfer of the optical strength from the L features to the exciton (X) and trion (T) implies that the exciton and trion are related to essentially free states, whereas the L features are related to strongly localized states. Note that for all optically active complexes some form of localization (on various monolayer imperfections, e.g., monolayer's local tension or shallow impurities) is generally expected. This confinement may be strong or weak. Here, by the designation of 'essentially free' states, we refer to those for which localization has insignificant effect on the emission energy, in contrast to the truly 'localized' states.

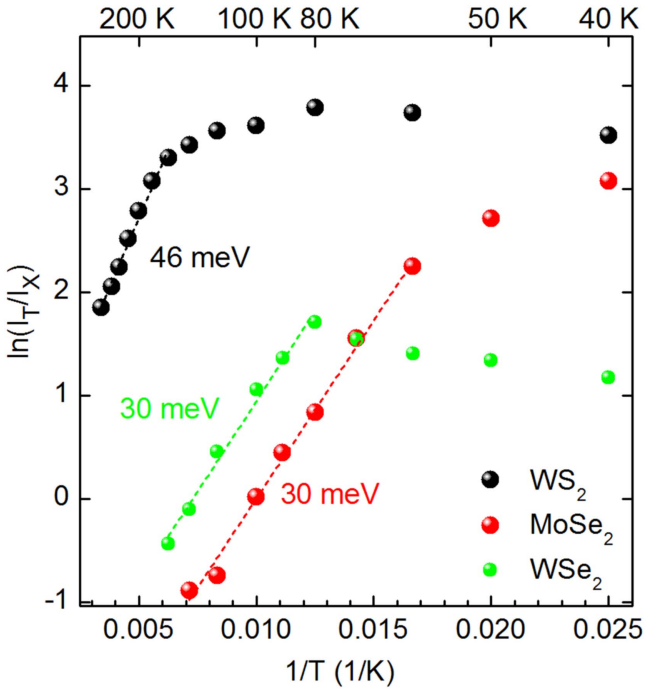

Figure 10. Integrated PL intensity rate $\ln(I_T/I_X)$ of the trion (T) and exciton (X) lines as a function of $1/T$ (symbols) for WS_2 (black), WSe_2 (green) and $MoSe_2$ (red). The lines are linear fits used to deduce the activation energies (see equation (1)).

At elevated temperatures, with the increase in the temperature in both the RC and PL spectra of WSe_2, WS_2 and $MoSe_2$ the transfer of spectral weight from trions to excitons is observed. To get a better insight into this process and to confirm our assignment of excitons X and trions T to the essentially free states, we have analyzed temperature evolution of the integrated PL intensity ratio of the trion and exciton lines. We perform a numerical fit to determine the exact shapes and the energy positions of the exciton and trion lines using the Lorentzian function. In figure 10 the logarithm of the trion to exciton ratio of integrated PL intensity is drawn as a function of invert temperature in WS_2, WSe_2 and $MoSe_2$. The data in figure 8 are presented only for those temperatures, for which the X and T peaks are well resolved and the fitting is reliable. For MoS_2 the data are not presented since in this monolayer the X line is not well resolved in the PL spectra. In the regime of higher T the temperature evolution of the total PL intensity of the trion and exciton lines ($I_T(T)$ and $I_X(T)$, respectively) can be described using the Boltzmann law:

$$I_T(T)/I_X(T) = \alpha_T/\alpha_X \exp -(E_T - E_X)/k_B T, \qquad (1)$$

where α_T and α_X are the trion and exciton degeneracies, E_T and E_X are their energy positions in the PL spectra, and k_B is the Boltzman constant. The energies obtained from equation (1), $\Delta E = 46$, 30, and 30 meV for WS_2, WSe_2 and $MoSe_2$, respectively, are in good agreement with the energy separation of the T and X lines in the PL spectra, which are equal to 42, 30 and 30 meV for WS_2, WSe_2 and $MoSe_2$, respectively (see figure 1).

As is seen from figure 10, the ratio of the exciton to trion PL intensity obeys Boltzmann law in WSe_2 at temperatures above $T \geqslant 80$ K, when the L lines disappear from the PL spectra (see figure 3(a)). In contrast, in WS_2, where the L lines disappear from the PL spectra in the same temperature range (see figures 6(c) and 9), the ratio of the exciton to trion PL intensity obeys Boltzmann law at much higher temperatures $T \geqslant 180$ K. In $MoSe_2$, where no additional lines, except X and T, are observed in the PL spectra (see Figure 7(a)), equation (1) for the X and T lines is valid at $T \geqslant 60$ K. This result reveals a complex interplay between the effect of different recombination channels (radiative and non-radiative) and 2D carrier concentration, which can be additionally dependent on position on the sample. However, in high temperature regime, different for different samples, radiative recombination of the trion and exciton are the dominant recombination channels. Significant difference in the energy separation of the trion and exciton lines in the PL spectra of selenides and sulfides are related to a strong difference in their 2D carrier concentration. In selenides, WSe_2 and $MoSe_2$, the carrier concentration is low and the energy separation of the X and T lines is equal to the trion binding energy. However, in WS_2 and MoS_2, the 2D electron concentration is high, which causes that during the radiative recombination of an electron–hole pair in a trion complex, an additional electron is excited over the Fermi energy due to the space filling effect, and the relation between the exciton and trion positions in the PL spectra is given by the formula [24]:

$$E_X - E_T = E_{b,T} + E_F, \qquad (2)$$

where $E_{b,T}$ is the trion binding energy and E_F is the Fermi energy. In order to determine the trion binding energy one has to decrease the 2D carrier concentration, what can be realized in a gated structure.

Lacking capabilities to conduct transport measurements on our monolayers we performed the following additional PL experiment from which we evaluated both the trion binding energy and the 2DEG concentration in WS_2 to show that the 2DCG concentration is substantially higher in the sulfides than in the selenides. It is well established that under ambient conditions the physisorbed O_2 and H_2O molecules deplete n-type materials such as MoS_2 and WS_2, much more than conventional electric field gating [39, 40]. In figure 11 we compare the RC and PL spectra recorded at $T = 295$ K in ambient and vacuum conditions for all the studied monolayers. The experiments were performed under the same conditions for all the samples. In the sulfides, WS_2 and MoS_2, the shape and energy position of the PL lines and RC resonances strongly differ between experiments performed in ambient and vacuum, which, as we will show, confirms the previous reports that in ambient the 2DCG concentration is strongly depleted. The PL spectra of WS_2 and MoS_2 measured in vacuum are dominated by the trion. However, in the PL spectra of WS_2 measured in ambient well resolved peaks of X and T are resolved. Their energy separation equal to 30 meV matches the trion binding energy reported in previous studies [14, 25, 26]. Having established the trion binding energy, we evaluate from the equation (1) and the energy separation of the X and T peaks in PL spectra measured at low temperatures in vacuum (see figure 2(b)) the Fermi energy

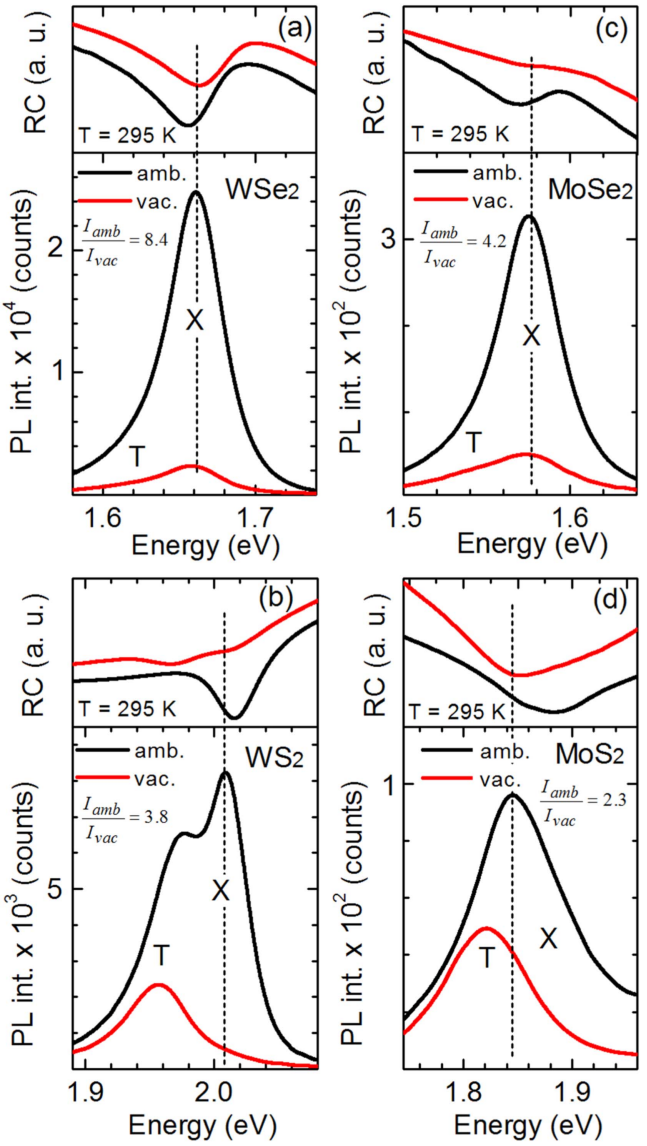

Figure 11. The PL spectra recorded at $T = 295$ K in ambient (black line) and vacuum (red line) for (a) WSe_2, (b) WS_2, (c) $MoSe_2$ and (d) MoS_2.

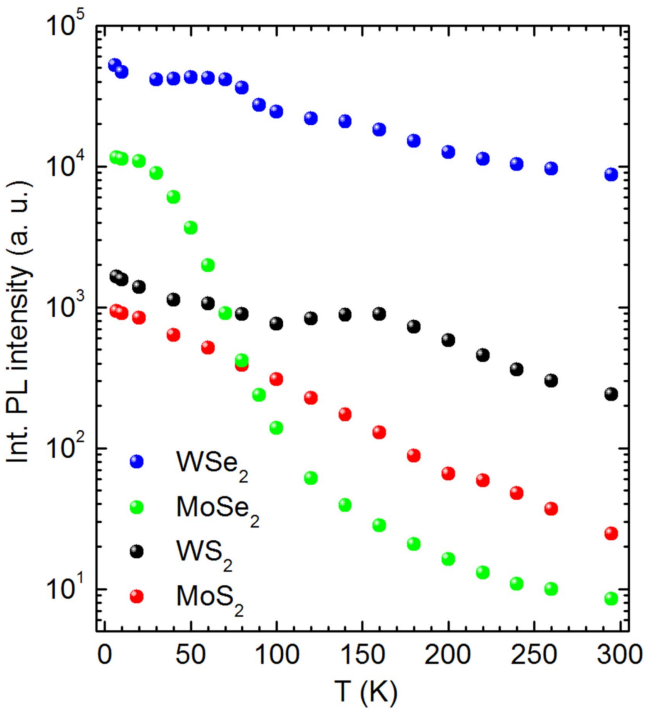

Figure 12. The temperature evolution of the total PL intensity in WSe_2, WS_2, $MoSe_2$ and MoS_2 monolayers.

$E_F = 12$ meV. Then, using the equation $n = m_e E_F/\pi\hbar^2$ and the electron effective mass $m_e = 0.37$ [6] we calculated the intrinsic 2D electron concentration $n = 1.86 \times 10^{12}$ cm^{-2}. In the PL spectra of MoS_2 measured in ambient we detect only the T line, which enables us to evaluate the trion binding energy. This observation also shows the high 2D electron gas concentration in MoS_2, even in vacuum. Using the theoretically calculated trion binding energy in MoS_2: $E_{b,T} = 30$ meV [36] and the electron effective mass of $m_e = 0.35$ [41], we evaluate the Fermi energy as $E_F = 13$ meV and the intrinsic 2D electron concentration as $n = 1.91 \times 10^{12}$ cm^{-2}.

As is seen in figures 11(a) and (c), in the PL and RC spectra of selenides, WSe_2 and $MoSe_2$, recorded at $T = 295$ K, in ambient and in vacuum, only one line of the exciton is detected in both monolayers. The energy position of the X line in the PL and RC spectra in both monolayers is almost the same. This observation confirms that the 2DCG concentration is substantially lower in the selenides than in the sulfides. Additionally, we find that in all the samples the PL intensity is substantially stronger in ambient than in vacuum, which confirms the previous reports [39, 40].

In figure 12 the evolution of the total PL intensity for all the monolayers is presented. At all the measured temperatures the total PL intensity is the highest in WSe_2. Also, we observe the decrease of the PL intensity with the increase in temperature for all the monolayers. However, this decrease is weak in WSe_2 (≈5×) and WS_2 (≈7×), strong in MoS_2 (≈40×) and dramatic in $MoSe_2$ (≈1000×). The temperature decrease of the PL intensity in WSe_2 is in contrast to the previous studies [42, 43], where the increase in the PL intensity of WSe_2 with increase in temperature was reported. Additionally, in [43], in which the authors compared the PL intensities of monolayers exfoliated onto the same substrate (as in this study), the PL intensity of $MoSe_2$ was higher than in WSe_2 at low temperatures and lower at higher temperatures. This contrasting behavior of the PL intensity of WSe_2 and $MoSe_2$ in our studies and in the previous reports is likely related to different concentration of the 2DCG. In [42] the authors performed comparative studies of the total intensity of both the suspended and gated WSe_2 and $MoSe_2$ monolayers, near the neutrality points, for a very low carrier concentration, whereas in our studies of intrinsic monolayers, even in the selenides, the 2DCG concentrations are substantial, of an order of 10^{10} cm^{-2} [16], which is evidenced by efficient trion emission even at elevated temperatures (see figures 3(a) and 6(a)).

4. Conclusion

To conclude, we present detailed temperature dependent ($T = 7$–295 K) optical spectroscopy studies of WSe_2, WS_2, $MoSe_2$ and MoS_2 monolayers exfoliated onto the same SiO_2/Si substrate. In the high energy region of the absorption type (reflectivity contrast) and emission (photo-luminescence) spectra of all the monolayer, the resonances related to the neutral and charged excitons (X and T) are detected in the entire measured temperature range. In the absorption spectra of WS_2 monolayer we reveal resonances arising from one neutral exciton and two negatively charged excitons. In the low energy PL spectra of WSe_2 and WS_2 we detect a group of lines (L), which dominates the spectra at low temperatures but rapidly quenches with the increase in temperature. We propose that the line interpreted previously in the PL spectra of WSe_2 and WS_2 as related to biexciton emission is a superposition of the biexciton, trion and localized exciton emission. We find that the total PL intensity at all the measured temperatures is the highest in WSe_2. We also observe that with the temperature increase from 7 to 295 K the total PL intensity decreases moderately in WSe_2 ($\approx 5\times$) and WS_2 ($\approx 7\times$), strongly in MoS_2 ($\approx 40\times$) and dramatically in $MoSe_2$ ($\approx 1000\times$).

Acknowledgments

This work was partly supported by the Polish NCN Grant No. 2013/09/B/ST3/02528, the Polish-Taiwanese Joint Research OSTMED PL-TWII/5/2015, Polish NCN Grant 'Maestro' No 2014/14/A/ST3/00654, and Polish NCN Grant Sonata No. 2013/11/D/ST3/02703.

References

[1] Mak K F, Lee C, Hone J, Shan J and Heinz T F 2010 Atomically thin MoS_2: a new direct-gap semiconductor *Phys. Rev. Lett.* **105** 136805
[2] Splendiani A *et al* 2010 Emerging photoluminescence in monolayer MoS_2 *Nano Lett.* **10** 1271–5
[3] Eda G, Yamaguchi H, Voiry D, Fujita T, Chen M and Chhowalla M 2011 Photoluminescence from chemically exfoliated MoS_2 *Nano Lett.* **11** 5111–6
[4] Radisavljevic B, Radenovic A, Brivio J, Giacometti V and Kis A 2011 Single-layer MoS_2 transistors *Nat. Nanotechnol.* **6** 147–50
[5] Zhang Y *et al* 2014 Direct observation of the transition from indirect to direct bandgap in atomically thin epitaxial $MoSe_2$ *Nat. Nanotechnol.* **9** 111–5
[6] Xiao D, Liu G B, Feng W, Xu X and Yao W 2012 Coupled spin and valley physics in monolayers of MoS_2 and other group VI dichalcogenides *Phys. Rev. Lett.* **108** 196802
[7] Cao T *et al* 2012 Valley-selective circular dichroism in MoS_2 *Nat. Commun.* **3** 887
[8] Sallen G *et al* 2012 Robust optical emission polarization in MoS_2 monolayers through selective valley excitation *Phys. Rev.* B **86** 081301
[9] Mak K F, He K L, Shan J and Heinz T F 2012 Control of valley polarization in monolayer MoS_2 by optical helicity *Nat. Nanotechnol.* **7** 494–8
[10] Wang Q H, Kalantar-Zadeh K, Kis A, Coleman J N and Strano M S 2012 Electronics and optoelectronics of two-dimensional transition metal dichalcogenides *Nat. Nanotechnol.* **7** 699–712
[11] Xu X, Xiao D, Heinz T F and Yao W 2014 Spin and pseudospins in layered transition metal dichalcogenides *Nat. Phys.* **10** 343–50
[12] Zhang Y J, Oka T, Suzuki R, Ye J T and Iwasa Y 2014 Electrically switchable chiral light-emitting transistor *Science* **344** 725–8
[13] He K, Kumar N, Zhao L, Wang Z, Mak K F, Zhao H and Shan J 2014 Tightly bound excitons in monolayer WSe_2 *Phys. Rev. Lett.* **113** 026803
[14] Chernikov A, Berkelbach T C, Hill H M, Rigosi A, Li Y, Aslan O B, Reichman D R, Hybertsen M S and Heinz T F 2014 Exciton binding energy and nonhydrogenic Rydberg series in monolayer WS_2 *Phys. Rev. Lett.* **113** 076802
[15] Ye Z, Cao T, O'Brien K, Zhu H, Yin X, Wang Y, Louie S G and Zhang X 2014 Probing excitonic dark states in single-layer tungsten disulphide *Nature* **513** 214–8
[16] Ross J S *et al* 2013 Electrical control of neutral and charged excitons in a monolayer semiconductor *Nat. Commun.* **4** 1474
[17] Withers F *et al* 2015 WSe_2 light-emitting tunneling transistors with enhanced brightness at room temperature *Nano Lett.* **15** 8223–8
[18] Wang G, Bouet L, Lagarde D, Vidal M, Balocchi A, Amand, Marie X and Urbaszek B 2014 Magneto-optics in transition metal diselenide monolayers *Phys. Rev.* B **90** 075413
[19] Arora A, Koperski M, Nogajewski K, Marcus J, Faugeras C and Potemski M 2015 Exciton band structure in layered WSe_2: from a monolayer to the bulk limit *Nanoscale* **7** 10421–9
[20] Wang G, Palleau E, Amand T, Tongay S, Marie X and Urbaszek B 2015 Polarization and time-resolved photoluminescence spectroscopy of excitons in $MoSe_2$ monolayers *Appl. Phys. Lett.* **106** 112101
[21] Godde T *et al* 2016 Exciton and trion dynamics in atomically thin $MoSe_2$ and WSe_2: effect of localization *Phys. Rev.* B **94** 165301
[22] Jadczak J, Delgado A, Bryja L, Huang Y S and Hawrylak P 2017 Robust high-temperature trion emission in monolayers of $Mo(S_ySe_{1-y})_2$ alloys *Phys. Rev.* B **95** 195427
[23] Mitioglu A A, Plochocka P, Jadczak J N, Escoffier W, Rikken G L J A, Kulyuk L and Maude D K 2013 Optical manipulation of the exciton charge state in single-layer tungsten disulfide *Phys. Rev.* B **88** 245403
[24] Mak K F, He K, Lee C, Lee G H, Hone J, Heinz T F and Shan J 2013 Tightly bound trions in monolayer MoS_2 *Nat. Mater.* **12** 207–11
[25] Plechinger G, Nagler P, Kraus J, Paradiso N, Strunk C, Schüller C and Korn T 2015 Identification of excitons, trions and biexcitons in single-layer WS_2 *Phys. Status Solidi* **9** 457–61
[26] Plechinger G *et al* 2016 Trion fine structure and coupled spin–valley dynamics in monolayer tungsten disulfide *Nat. Commun.* **7** 12715
[27] You Y, Zhang X X, Berkelbach T C, Hybertsen M S, Reichman D R and Heinz T F 2015 Observation of biexcitons in monolayer WSe_2 *Nat. Phys.* **11** 477–81
[28] Jones A M *et al* 2013 Optical generation of excitonic valley coherence in monolayer WSe_2 *Nat. Nanotechnol.* **8** 634–8
[29] Molas M, Faugeras C, Slobodeniuk A O, Nogajewski K, Bartos M, Basko D M and Potemski M 2017 Brightening of dark excitons in monolayers of semiconducting transition metal dichalcogenides *2D Mater.* **4** 021003

[30] Zhu Z Y, Cheng Y C and Schwingenschlogl U 2011 *Phys. Rev.* **84** 153402
[31] Dery H and Song Y 2015 Polarization analysis of excitons in monolayer and bilayer transition-metal dichalcogenides *Phys. Rev.* B **92** 125431
[32] Komsa H-P and Krasheninnikov A V 2015 Native defects in bulk and monolayer MoS_2 from first principles *Phys. Rev.* B **91** 125304
[33] Lin Y-C *et al* 2015 Three-fold rotational defects in two-dimensional transition metal dichalcogenides *Nat. Commun.* **6** 6736
[34] Gladysiewicz A, Bryja L, Wójs A and Potemski M 2006 Effect of free carriers and impurities on the density of states and optical spectra of two-dimensional magnetoexcitons *Phys. Rev.* B **74** 115332
[35] Jadczak J, Bryja L, Wójs A and Potemski M 2012 Optically induced charge conversion of coexistent free and bound excitonic complexes in two-beam magneto-photoluminescence of two-dimensional quantum structures *Phys. Rev.* B **85** 195108
[36] Ganchev B, Drummond N, Aleiner I and Falko V 2015 Three-particle complexes in two-dimensional semiconductors *Phys. Rev. Lett.* **114** 107401
[37] Schmidt T and Lischka K 1992 Excitation-power dependence of the near-band-edge photoluminescence of semiconductors *Phys. Rev.* B **45** 8989
[38] Taguchi T, Shirafuji J and Inuishi Y 1975 Excitonic emission in cadmium telluride *Phys. Status Solidi* B **68** 727
[39] Tongay S, Zhou J, Ataca C, Liu J, Kang J S, Matthews T S, You L, Li J, Grossman J C and Wu J 2013 Broad-range modulation of light emission in two-dimensional semiconductors by molecular physisorption gating *Nano Lett.* **13** 2831–6
[40] Miller B, Parzinger E, Vernickel A, Holleitner A W and Wurstbauer U 2015 Photogating of mono- and few-layer MoS_2 *Appl. Phys. Lett.* **106** 122103
[41] Cheiwchanchamnangij T and Lambrecht W R L 2012 Quasiparticle band structure calculation of monolayer, bilayer, and bulk MoS_2 *Phys. Rev.* B **85** 205302
[42] Zhang X X, You Y, Zhao S Y F and Heinz T F 2015 Experimental evidence for dark excitons in monolayer WSe_2 *Phys. Rev. Lett.* **115** 257403
[43] Wang G *et al* 2015 Spin–orbit engineering in transition metal dichalcogenide alloy monolayers *Nat. Commun.* **6** 10110